COBEM 2021 Florianópolis - Brasil
ABCM Associação Brasileira de Engenharia e Ciências Mecânicas
26th ABCM International Congress of Mechanical Engineering
November 22-26, 2021. Florianópolis, SC, Brazil

COB-2021-0161
EFFECTS OF INPUT TEMPERATURE PROFILE IN THE DESIGN OF CONTINUOUS-FLOW SENSIBLE-THERMAL ENERGY STORAGE SYSTEMS

Conrado Ermel
Paulo S. Schneider
Universidade Federal do Rio Grande do Sul - UFRGS, Brazil
conradoermel@gmail.com

Marcus V.A. Bianchi
National Renewable Energy Laboratory - NREL, USA

Abstract. *Several thermal processes require a stable temperature profile to be effective. Thermal energy storage stands as a promising technology to stabilize such processes, having been widely employed for short and long-time storage, from small domestic solutions up to large facilities used to support renewables intermittency. The design of Thermal Energy Storage Systems (TESS) is still challenging, no matter the chosen technology. The present work considers the influence of different input temperature profiles on the operation and design of continuous-flow sensible-TESS. By using a Lumped Element Model (LEM) and a design optimization procedure, we determined the impact of the energy source characteristics on the operation and the geometrical arrangement of a TESS. Preliminary results revealed that the thermal amplitude of the studied TES is augmented by* 24 % *when switching from a sinusoidal temperature profile to a Heaviside step function signal. Such deviation indicates the relevance of considering the input temperature profile in TESS design, in addition to other common parameters such as the system power, energy density, and capacity.*

Keywords: *Thermal Energy Storage, TES, Sensible Heat, TES Design, Temperature profile.*

1. INTRODUCTION

The world is facing a climate challenge, and pursuing a smarter use of natural resources is imperative (Masson-Delmotte *et al.*, 2021). Thermal Energy Storage (TES) is a key technology capable of supporting energy management both on generation and demand sides (Brückner *et al.*, 2015). On the generation side, thermal storage can leverage the widespread of renewables by balancing the energy surplus and peak demands. As renewables are expected to grow from 15 % of total generation in 2015 to 63 % in 2050 Gielen *et al.* (2019), and their power output is intermittent and not fully predictable (Yekini Suberu *et al.*, 2014), TES will be relevant to this transition towards a cleaner energy mix (Alva *et al.*, 2018). In Concentrated Solar Power (CSP) power plants, for instance, it can improve the system performance and make it more dispatchable (Alobaidd *et al.*, 2016).

On the demand side, TES may be used as an energy management tool to reduce waste, and increase the efficiency of several industrial processes (Sarbu and Sebarchievici, 2018). In buildings, TES may be used to regulate thermal loads as a passive component installed in the building envelope (Kishore *et al.*, 2020). Heating, Ventilation, and Air Conditioning (HVAC) is also a suitable application for TES, for it can be used in night ventilation (Solgi *et al.*, 2018), or treatment of the air before entering the HVAC system (Farah *et al.*, 2019), among several other applications. Depending on the application, the thermal storage device can operate in batches where it is charged and discharged in different moments, or it can be continuously fed with a heat-transfer-fluid (Andriotty *et al.*, 2019).

The selection and sizing of thermal storage devices are complex and can be accomplished by different approaches. The difficulty is due to the varied phenomena involved, the need for evaluating the system over time, and other relevant aspects. Computational Fluid Dynamics (CFD) simulations of TES systems were explored by different authors who tried to understand the system's behavior (Tay *et al.*, 2013; Parsazadeh and Duan, 2018). Nonetheless, CFD simulations of thermal storage systems are sometimes prohibitive, for the simulation must be performed for each time step to capture the transient behavior. Despite the efforts to reduce the high computational effort of TES CFD-simulations (Pizzolato *et al.*, 2015), the time needed to reach a solution may sometimes prevent the use of CFD in TESS engineering. Zero-dimensional energy models are a common alternative to simulate TES in time. While works like the one of Farah *et al.* (2019) employ commercial software like TRNSYS to perform the simulations, others choose to developed energy models based on linear programming (Andriotty *et al.*, 2016). The design and optimization of thermal storage is often a hand-tailored task. In other words, there is not a general method to select, size, and optimize a TES system.

The present paper focuses on the design and optimization of a particular TESS, the Continuous-Flow Sensible-TES (CFSTES) which consists of a passive device containing thermal storage material. Air flows through it continuously charging and discharging the device Andriotty (2018). This system can be adopted in any situation where a fluid with oscillating temperature must have its thermal amplitude attenuated. Passive TESS such as the one CFSTES can help temperature control in building applications, automobiles, textiles, food & drug shipping (Alva *et al.*, 2018). Moreover, it can be particularly useful for HVAC like the one studied by Farah *et al.* (2019), where energy savings up to $14\,\%$ were reported.

Regarding sizing and optimization of CFSTES, an alternative to solutions based on CFD was proposed by Andriotty *et al.* (2020). The authors presented an optimization method with the mass of storage material as the objective function. Dimensionless relations of the system's NTU and oscillation period were presented, turning the method into a guide for the engineering design of CFSTES. Although proposing a novel approach for TES design and sizing, the authors focused only on heat sources with a sinusoidal oscillating temperature. Hence potential applications with different temperature profiles like Heaviside or triangular shapes cannot yet adopt the proposed method. Therefore, in the present paper, we evaluated the adoption of the optimization method proposed by Andriotty *et al.* (2020) in applications with temperature input profiles different than sinusoidal ones. If the method works for other temperature profiles, a new set of applications like industrial waste heat or HVAC could adopt the method for CFSTES design. The main goal is to determine if the method is suitable for triangular and Heaviside profiles, or if new correlations must be explored.

2. METHODOLOGY

This paper explores a special kind of CFSTES, which previous authors named Thermal Rectifier (TR). The system under discussion uses sensible heat storage material to exchange thermal energy with an air stream. It was previously explored by Andriotty *et al.* (2016) and has the main objective of reducing the thermal amplitude of the air stream with a cyclic temperature profile, such as the one presented in Fig. 1. The authors used a sinusoidal temperature profile as a

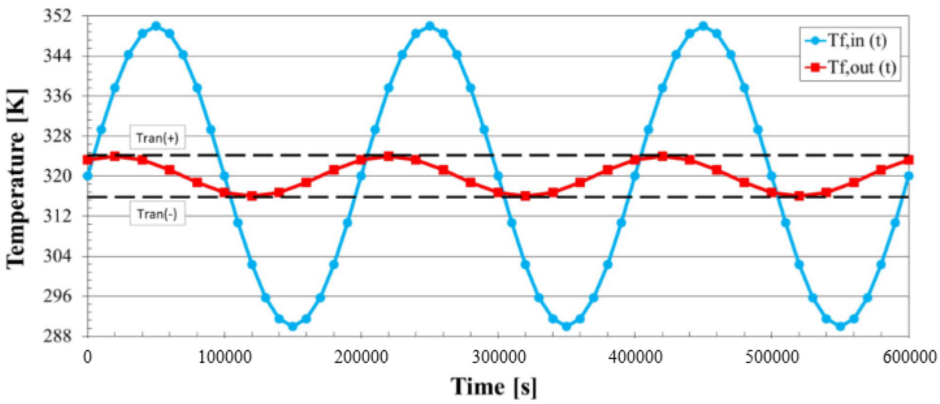

Figure 1: Temperature profile in a rectifier-TESS. Blue curve: input temperature; Red curve: output temperature (ANDRIOTTY, T.H; SCHNEIDER; RODRIGUES, 2020)

reference. Hence, the system operates with a fixed airflow rate, with the input temperature varying according to the blue line. The maximum and minimum temperature in the system output is reduced as observed in the red line. In other words, the stream thermal amplitude is modulated (reduced) to a new range.

The CFSTES presented in Fig. 2 was considered for the simulations performed. The system is composed of several layers of sensible energy storage material. Air flows through the channels and heat is exchanged between the fluid and solid sheets. In this arrangement the controllable parameters are the system length L, width W, the thickness of the solid sheet e_f, and channel thickness e_f, that is the space between sheets.

2.1 Mathematical equations

The first step was developing a mathematical model capable of representing the physical phenomena involved in the system of Fig. 2. The model takes into consideration the heat transfer between the air and the solid sheets, which occurs whenever a temperature gradient exists between them. The mathematical modeling considered the symmetry planes, as presented in Fig. 3, therefore, conservation equations were developed for each solid-fluid domain pair. Heat transfer between the fluid and solid domain was analyzed for each symmetry plane. By considering the thermophysical properties of the solid and fluid phase, and neglecting radiation heat transfer, the energy balance of the system can be described by

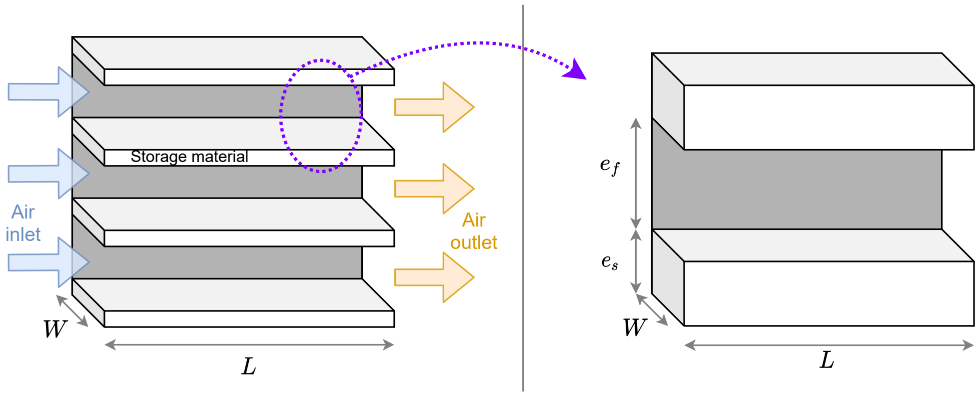

Figure 2: Studied CFSTES (container with the continuous fluid flow).

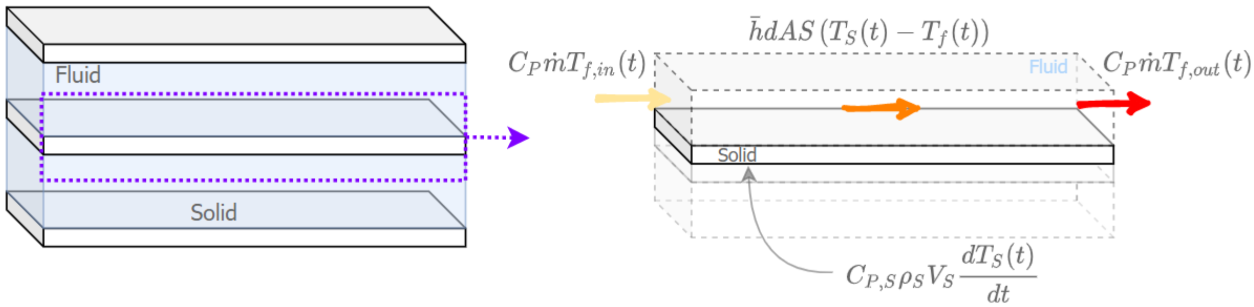

Figure 3: Energy balance and control volume analyzed in the generic TESS.

Eq. (1) for the solid energy material, and by Eq. (2) for the fluid phase.

$$\rho_s C_{p,s} V_s \frac{dT_s(t)}{dt} = -\bar{h}dA_s\left(T_s(t) - \bar{T}_f(t)\right), \tag{1}$$

where ρ_s, $C_{p,s}$, and V_s are the solid specific mass $\mathrm{kg/m^3}$, specific heat $\mathrm{kJ/(kg\,K)}$, and volume $\mathrm{m^3}$, respectively. Term $T_s(t)$ is the solid temperature at the time (t), dA_s is the solid interface area $\mathrm{m^2}$, and $\bar{T}_f(t)$ is the fluid average temperature in [K] at a given time. In the fluid energy balance

$$\rho_f\, C_{p,f}\, V_f \frac{dT_{f,x}(t)}{dt} = \dot{m}\, C_{p,f}\, T_{f,in}\,(t) -\, \dot{m}\, C_{p,f} T_{f,out}\,(t) + \bar{h}\, dA_s\left(T_s\,(t) -\, \overline{T}_f\,(t)\right), \tag{2}$$

ρ_f stands for the fluid specific mass $\mathrm{kg/m^3}$, $C_{p,f}$ is the fluid specific heat $\mathrm{kJ/(kg\,K)}$, and V_f is the fluid volume in $\mathrm{m^3}$. The fluid temperature in position (x) in time (t) is given by $dT_{f,x}(t)$. Term $\dot{m}$ represents the fluid mass flow rate $\mathrm{kg/s}$, while $T_{f,out}(t)$ is the fluid temperature in the system outlet. In both Eq.(1) and Eq.(2), the average convective heat transfer coefficient $\bar{h}$, in $\mathrm{W/(m^2\,K)}$ was determined from the Nusselt correlation

$$Nu_{0-x} = 7.55 + \frac{0.024x_*^{-1.14}}{1 + 0.0358Pr^{0.17}x_*^{-0.64}}, \tag{3}$$

that is recommended for parallel-plate channels in the range of 0.1 < Pr < 1000 (Adrian Bejan, 2013, p. 128). The system was divided into N cells, in the x-direction, as represented in Fig. 4. Hence, the energy conservation equations were applied to each cell.

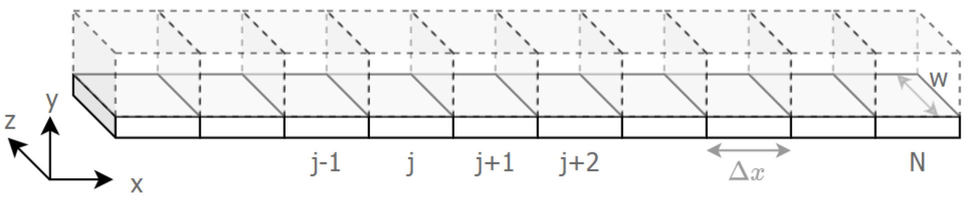

Figure 4: Division of the plate in N cells. Two-dimensional analysis, considering W=1.

The solution of the equation system was achieved by adopting the Lumped Element Model (LEM). This method is suitable for a thermal energy storage system, considering its physical characteristics and transient heat conduction (Li *et al.*, 2012; Yuan *et al.*, 2015). The solution is derived from the consideration of a constant and uniform temperature in the solid material, hence, a simplified solution is assumed to determine the fluid temperature in the outlet (Andriotty *et al.*, 2019). From the energy balance, it is then possible to define a solution based on the LEM, as presented by Andriotty *et al.* (2016), to arrive at two main equations. The solid temperature is represented by Eq.(4), which considers the solid heat capacity, the main heat transfer mechanisms, and an average fluid temperature.

$$T_s(t) = T_{s,i} - \left[1 - \, exp\left(-\frac{\bar{h}A_s}{C_{p,s}\rho_s V_s}t\right)\right](T_{s,i} - \overline{T}_f(t))\,. \tag{4}$$

This average temperature, $\overline{T}_f(t)$, is defined by Eq.(5), where the temperature of the j and $j-1$ volumes are considered.

$$\overline{T}_{f,j}(t) = \frac{T_{f,j-1}(t) + T_{f,j}(t)}{2}. \tag{5}$$

The fluid temperature in the system output at a given time, $T_{f,out}(t)$, can then be determined by Eq.(6).

$$T_{f,out}(t) = T_s(t) - \left[exp\left(-\frac{\bar{h}A_s}{\dot{m}c_{p,f}}\right)(T_s(t) - \, T_{f,in}(t))\right], \tag{6}$$

Once Eq. (4), (5), and (6) are applied to each j cell represented in Fig. 4, it is possible to determine the fluid and solid temperatures at a given instant t, at any length of the system, including the fluid output temperature. The total heat transfer for the whole TESS can be estimated by adding the contribution of each section.

2.2 Optimization Algorithm

Once the system was represented by the proposed mathematical model, the second step was developed: the TESS design methodology routine, also named optimization algorithm. The main objective of the proposed methodology is to find the possible geometrical configuration for the TESS under consideration, when it is subject to a given input temperature profile, so it can deliver a predetermined thermal amplitude in the system output. The methodology was based on an Inverse Problem Philosophy (IPP) to serve as a TESS design tool, capable of considering input and output constraints.

The relatively fast results provided by the employed model allow for the use of simple optimization procedures. Even dividing the model into several volumes to enhance results accuracy, and evaluating the simulations in long time periods, the adopted model is still capable of compiling the results in less than five minutes. Therefore, observing the recommendations of Andriotty (2018), an exhaustive search technique was adopted to determine the optimal TESS design that assures the system to operate under the project requirements.

Figure 5 presents the solution methodology. First, the system parameters must be entered, followed by the maximum accepted thermal amplitude. Step two requires the user to define the range and increments of each of the variables that

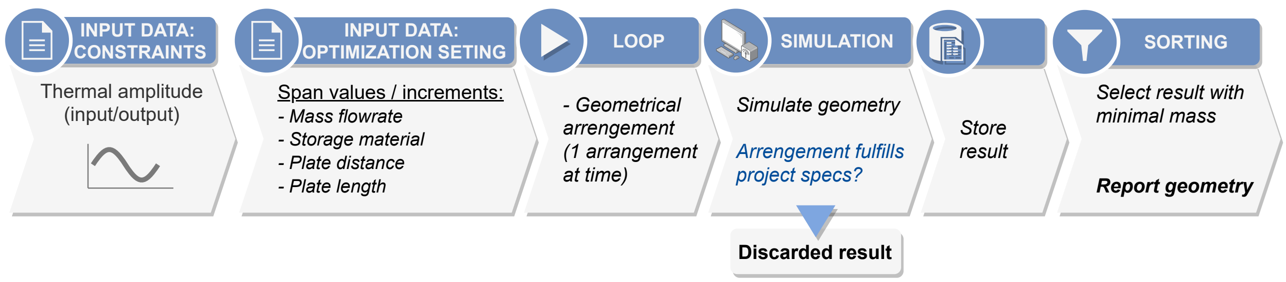

Figure 5: Methodology structure and optimization scheme.

can be changed in the system: air mass flow rate, storage material, plate distance, and plate thickness. At this point, the number of simulations is defined, since it is a function of all possible combinations among the parameters. A loop executes these simulations and for each result, tests if the designed system fulfills the project requirements (thermal amplitude in the output). If the configuration fails in the test, the result is discarded, if it passes the system configuration is stored. In the last step, the methodology sorts all the approved configuration and select the one with the minimal mass of storage material as the best design for the system.

3. RESULTS

3.1 Validation

Model validation was accomplished by comparing results with the study of Andriotty *et al.* (2020). The authors presented a CFD analysis of the system of Fig. 2, using air as heat transfer fluid and AISI 304 as storage material. The materials' properties are presented in Tab. 1. The air temperature ranged from 360 K to 440 K, following a sinusoidal signal with 30 000 s and 10 s of time-step. The TES simulated by Andriotty (2018) has a single channel of e_f=46.6 mm

Table 1: Parameters adopted in the simulation (Andriotty, 2018).

Fluid$^{(1)}$

Parameter	*Value*	*Unit*
Cp_f	1008	[kJ/kg]
rho_f	1.103	[kg/m^3]
k_f	0.02785	[W/(m K)]

Solid$^{(2)}$

Parameter	*Value*	*Unit*
Cp_s	300	[kJ/kg]
rho_s	3000	[kg/m^3]
k_s	14.9	[W/(m K)]

Time

Parameter	*Value*	*Unit*
Period	30000	[s]
Cycles	2	-
Timestep	10	[s]

Geometry

Parameter	*Value*	*Unit*
e_f	0.0466	[m]
e_s	0.02545	[m]
L	1	[m]
m	0.08	[kg/s]

$^{(1)}$ Properties of air (Andriotty, 2018).
$^{(2)}$ Heat storage material: AISI 304 (Andriotty, 2018)

and 1 m length. The AISI 304 sheets were 25.4 mm thick. The system was reproduced in the present paper for validation.

The validation results are displayed in Fig. 6. The blue signal represents the air temperature in the system input, while the temperature in the output is represented by the red line. The rectifier effect on the thermal amplitude is observed as it decreases from 80 K in the system input to 61.6 K in the output. The results from the work of Andriotty *et al.* (2020)

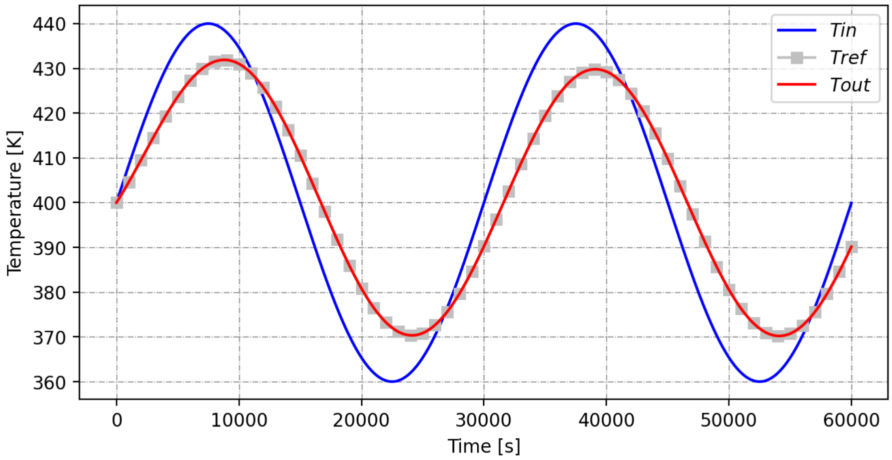

Figure 6: Validation. Blue: Input temperature, Red: Simulation results for output temperature, Gray: Reference data for validation (Andriotty *et al.*, 2020).

are presented in gray. Deviations between the reference data and the model results indicate almost perfect agreement as the deviation absolute average was 8.2×10^{-4} %. The validation results suggest the model capability of representing the operation of sensible TESS operation under continuous flow, allowing for further evaluations.

3.2 Model Response to Different Input Temperature Profiles

The influence of different input temperature profiles on the model results was assessed. The first analysis was executed using a sinusoidal temperature profile. It is possible to observe in Fig. 7a that the fluid thermal amplitude in the system input (green) is significantly reduced in the system output (blue line). The output temperature profile still follows a sinusoidal signal, which is expected since the lumped element model Eq. (4), (5), and (6), is based on exponential equations. When a linear temperature profile is imposed, the system response is delayed, as observed in Fig. 7b. After a stabilization time, the temperature slope of the outlet temperature equals the one of the inlet. This trend demonstrates that when short-time variations occur the system acts as a buffer, absorbing the fluctuations.

Figure8a shows the system response when a triangular temperature is present in the input. Finally, a Heaviside profile was tested in the model, Fig. 8b. It is worth noticing that the abrupt decrease in the output temperature is due to the flow start. Since at time zero all the system is in equilibrium (400 K), when the fluid starts to flow, the output temperature

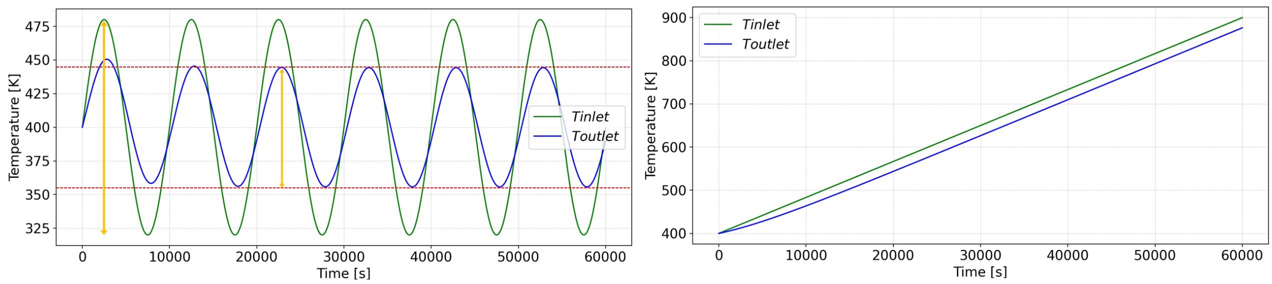

(a) (b)

Figure 7: Influence of temperature profiles in the system output temperature. a) Sinusoidal signal, b) Linear signal. Green lines are the input temperatures, and blue lines represent the output temperature.

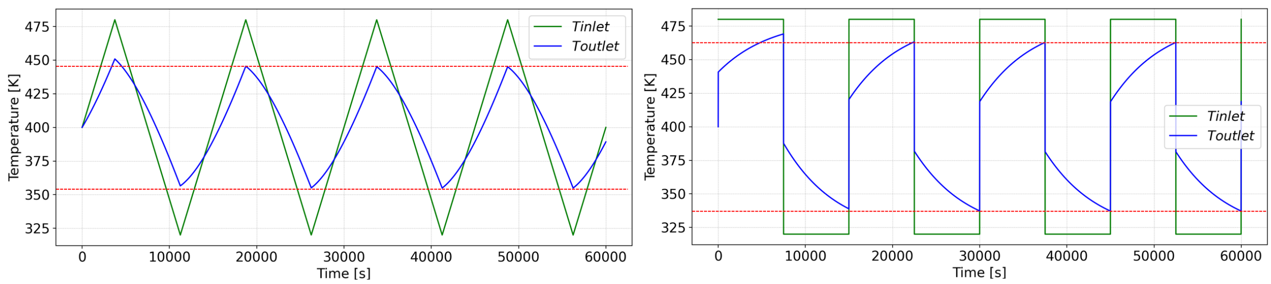

(a) (b)

Figure 8: Influence of temperature profiles in the system output temperature. a) Triangular signal, b) Heaviside signal. Green lines are the input temperatures, and blue lines represent the output temperature.

rapidly decreases.

If the system parameters are fixed, the system's outlet temperature changes with the input profile as presented by Tab. 2. Thermal amplitude is the difference between the maximum and the minimum temperature, and for a sinusoidal profile, the outlet amplitude was of $88.63\,\mathrm{K}$. Changing the input profile to a triangular signal causes the outlet amplitude to rise up to $90.09\,\mathrm{K}$, while the Heaviside signal shows an outlet amplitude of $125.62\,\mathrm{K}$. The maximum and minimum temperatures were measured after the system was stabilized, i.e. from $40\,000\,\mathrm{s}$ to $60\,000\,\mathrm{s}$.

Table 2: System output temperatures as a function of the input temperature profile.

Temp. profile (inlet)	T_{max} (outlet)	T_{min} (outlet)	Diff. in max temp.$^{(1)}$	Diff. in min temp.$^{(1)}$	Amplitude
Sinusoidal	444.31 K	355.68 K	-	-	88.63 K
Triangular	445.03 K	354.94 K	0.16%	-0.21%	90.09 K
Heaviside	462.81 K	337.19 K	4.00%	-5.00%	125.62 K

$^{(1)}$ Compared with the sinusoidal result.

4. DISCUSSIONS AND CONCLUSIONS

In this work, a simulation model of a Continuous-Flow Sensible-TES is presented. The model was previously proposed by Andriotty *et al.* (2020), however only to be applied to sinusoidal input temperature profiles. We have assessed the model behavior when operating with different input profiles like triangular and Heaviside signals, which may represent several waste heat applications in the industry, or in HVAC. Validation of the developed model was realized by comparing the model results with reference data from previous works.

The validation results indicate the system is capable of predicting the outlet temperature of the CFSTES if a sinusoidal oscillating signal is imposed on it. Different input profiles were assessed while keeping the same average temperature, thermal amplitude, frequency, and period for all cases simulated. When subject to a triangular signal, the system response regarding thermal amplitude was $0.37\,\%$ higher than the one predicted for a sinusoidal signal. Considering that the thermal rectifier is designed to guarantee a maximum thermal amplitude in the output, results suggest the changing the input temperature profile may influence the output thermal amplitude. Higher deviations were found when imposing a Heaviside signal to the system input. In this case, the thermal amplitude differs up to $9\,\%$ from the one of the sinusoidal signal. Since the main objective of the method proposed by Andriotty *et al.* (2020) is to determine the optimum geometrical arrangement of a CFSTES subject to sinusoidal signal, the deviations on thermal amplitude found in the present paper suggest that a new set of correlations must be developed if the method is to be used in triangular and Heaviside temperature profiles.

Further, we will adapt the LEM method to correctly describe triangular and Heaviside temperature profiles. Hence, the CFSTES design and optimization method will be extended for applications presenting such behavior. This will support the selection of proper geometrical arrangement of CFSTES also for those applications, helping engineers and TES designers.

5. ACKNOWLEDGMENTS

Conrado Ermel acknowledges CNPq - Conselho Nacional de Pesquisa e Desenvolvimento, for the financial support.

6. REFERENCES

Adrian Bejan, 2013. *CONVECTION HEAT TRANSFER*. John Wiley and Sons, Inc., Hoboken, NJ - USA, 4th edition. ISBN 978-0-470-90037-6.

Alobaidd, X., Mertensd, X., Starkloffd, X., Lanzd, X., Heinzed, X. and Eppled, X., 2016. "Progress in dynamic simulation of thermal power plants". *Progress in Energy and Combustion Science journal*, Vol. 59, pp. 79–162. doi:10.1016/j.pecs.2016.11.001. URL `https://ac.els-cdn.com/S0360128516300375/1-s2.0-S0360128516300375-main.pdf?_tid=bcf3f680-f78d-11e7-b248-00000aab0f6b&acdnat=1515757559_d897a77b4080b9739cde89a00fc72a0f`.

Alva, G., Lin, Y. and Fang, G., 2018. "An overview of thermal energy storage systems". *Energy*, Vol. 144, pp. 341–378. ISSN 03605442. doi:10.1016/j.energy.2017.12.037. URL `https://doi.org/10.1016/j.energy.2017.12.037`.

Andriotty, T., 2018. *PROJETO INVERSO APLICADO À MODELAGEM DE SISTEMAS DE ACUMULAÇÃO DE ENERGIA TÉRMICA SENSÍVEL*. Ph.D. thesis, Universidade Federal do Rio Grande do Sul. doi:10.1017/CBO9781107415324.004.

Andriotty, T., Rodrigues, L., Rocha, L.A. and Schneider, P., 2016. "Optimization of a sensible thermal storage system by a lumped approach". *Defect and Diffusion Forum*, Vol. 366, No. April, pp. 182–191. ISSN 16629507. doi:10.4028/www.scientific.net/DDF.366.182.

Andriotty, T., Schneider, P. and Rodrigues, L., 2020. "Accuracy of lumped element model for cyclic sensible thermal energy storage systems". *Journal of Energy Storage*, Vol. 28, No. February, p. 101277. ISSN 2352152X. doi:10.1016/j.est.2020.101277. URL `https://doi.org/10.1016/j.est.2020.101277`.

Andriotty, T.H., Smith Schneider, P. and Jenisch Rodrigues, L., 2019. "Inverse design methodology to optimize sensible thermal energy storage systems working as rectifiers". *International Journal of Energy Research*, Vol. 43, No. 12, pp. 6442–6453. ISSN 1099114X. doi:10.1002/er.4463.

Brückner, S., Liu, S., Miró, L., Radspieler, M., Cabeza, L.F. and Lävemann, E., 2015. "Industrial waste heat recovery technologies: An economic analysis of heat transformation technologies". *Applied Energy*, Vol. 151, pp. 157–167. ISSN 03062619. doi:10.1016/j.apenergy.2015.01.147.

Farah, S., Liu, M. and Saman, W., 2019. "Numerical investigation of phase change material thermal storage for space cooling". *Applied Energy*, Vol. 239, pp. 526–535. ISSN 03062619. doi:10.1016/j.apenergy.2019.01.197. URL `https://www.scopus.com/inward/record.uri?eid=2-s2.0-85061014593&doi=10.1016%2Fj.apenergy.2019.01.197&partnerID=40&md5=78011fe2a940037dce7c9fd3e31403fe`.

Gielen, D., Boshell, F., Saygin, D., Bazilian, M.D., Wagner, N. and Gorini, R., 2019. "The role of renewable energy in the global energy transformation". *Energy Strategy Reviews*, Vol. 24, pp. 38–50. ISSN 2211-467X. doi:10.1016/J.ESR.2019.01.006. URL `https://www.sciencedirect.com/science/article/pii/S2211467X19300082`.

Kishore, R.A., Bianchi, M.V., Booten, C., Vidal, J. and Jackson, R., 2020. "Optimizing PCM-integrated walls for potential energy savings in U.S. Buildings". *Energy and Buildings*, Vol. 226, p. 110355. ISSN 03787788. doi:10.1016/j.enbuild.2020.110355.

Li, P., Van Lew, J., Chan, C., Karaki, W., Stephens, J., and generalized analysis of efficiencies of thermal energy storage systems O'Brien, J.E., 2012. "Similarity and generalized analysis of efficiencies of thermal energy storage systems". *Renewable Energy*, Vol. 39, No. 1, pp. 388–402. ISSN 09601481. doi:10.1016/j.renene.2011.08.032. URL `http://dx.doi.org/10.1016/j.renene.2011.08.032`.

Masson-Delmotte, V., Zhai, P., Pirani, A., Connors, S., Péan, C., Berger, S., Caud, N., Chen, Y., Goldfarb, L., Gomis, M.I., Huang, M., Leitzell, K., Lonnoy, E., Matthews, J., Maycock, T., Waterfield, T., Yelekçi, O., Yu, R. and Zhou, B.e., 2021. "IPCC, 2021: Summary for Policymakers. In: Climate Change 2021: The Physical Science Basis. Contribution of Working Group I to the Sixth Assessment Report of the Intergovernmental Panel on Climate Change". Technical report, Cambridge University Press. In Press., Cambridge, Massachusetts.

Parsazadeh, M. and Duan, X., 2018. "Numerical study on the effects of fins and nanoparticles in a shell and tube phase change thermal energy storage unit". *Applied Energy*, Vol. 216, pp. 142–156. ISSN 03062619. doi:10.1016/j.apenergy.2018.02.052. URL https://linkinghub.elsevier.com/retrieve/pii/S0306261918301776.

Pizzolato, A., Donato, F., Verda, V. and Santarelli, M., 2015. "CFD-based reduced model for the simulation of thermocline thermal energy storage systems". *Applied Thermal Engineering*, Vol. 76, pp. 391–399. ISSN 13594311. doi:10.1016/j.applthermaleng.2014.11.029. URL http://dx.doi.org/10.1016/j.applthermaleng.2014.11.029.

Sarbu, I. and Sebarchievici, C., 2018. "A comprehensive review of thermal energy storage". *Sustainability (Switzerland)*, Vol. 10, No. 1. ISSN 20711050. doi:10.3390/su10010191.

Solgi, E., Hamedani, Z., Fernando, R., Skates, H. and Orji, N.E., 2018. "A literature review of night ventilation strategies in buildings". doi:10.1016/j.enbuild.2018.05.052.

Tay, N., Bruno, F. and Belusko, M., 2013. "Comparison of pinned and finned tubes in a phase change thermal energy storage system using CFD". *Applied Energy*, Vol. 104, pp. 79–86. ISSN 03062619. doi:10.1016/j.apenergy.2012.10.040. URL https://linkinghub.elsevier.com/retrieve/pii/S0306261912007593.

Yekini Suberu, M., Wazir Mustafa, M. and Bashir, N., 2014. "Energy storage systems for renewable energy power sector integration and mitigation of intermittency". *Renewable and Sustainable Energy Reviews*. ISSN 13640321. doi:10.1016/j.rser.2014.04.009. URL https://www.sciencedirect.com/science/article/pii/S1364032114002366?via%3Dihub.

Yuan, S., Zhou, J. and Hu, J., 2015. "A lumped element method for modeling the two-phase choking flow through hydraulic orifices". *International Journal of Heat and Mass Transfer*, Vol. 81, pp. 355–361. ISSN 00179310. doi:10.1016/j.ijheatmasstransfer.2014.10.045.

7. RESPONSIBILITY NOTICE

The authors are solely responsible for the printed material included in this paper.